

Activation of Methane on Iron, Nickel, and Platinum Surfaces.
A Molecular Orbital Study

Alfred B. Anderson and John J. Maloney

Chemistry Department, Case Western Reserve University
Cleveland, Ohio 44106

The activation of alkane CH bonds is the first step in hydrogenolysis and oxidation catalysis. It is clear from simple consideration of metal-hydrogen bond strengths (≈ 250 kJ/mol) and CH bond strengths (434 kJ/mol for breaking the first CH bond in methane) that oxidative addition and not hydrogen atom abstraction will be the route followed on metal surfaces. In contrast, O^- defect centers at oxide surfaces do abstract hydrogen atoms from methane, forming gas phase methyl radicals (1). The greater strength of an OH bond over a CH bond allows this to happen; a molecular orbital analysis has been published recently (2). Though kinetic studies of alkane reactions on metal surfaces are large in number, little is known about catalyst surface composition and structure or the structure and electronic factors responsible for CH activation by metals. The purpose of the present work is to explore mechanisms, activation energies, and orbital interactions associated with the oxidative addition of a methane CH bond to several idealized clean transition metal surfaces.

The metals chosen for our theoretical exploration, iron, nickel, and platinum, have been the topics of several systematic methane catalysis and surface science studies in recent years. A theoretical study of the oxidative addition of methane to an iron surface indicated the reaction was exothermic with an activation energy barrier of roughly 88 kJ/mol (3). In that study, low barriers were also found for dehydrogenation of CH_x ($x=1-3$) fragments and this is reflected in the ability of iron particles to catalyze the high temperature pyrolysis of natural gas to graphite fibers as studied recently by Tibbetts (4). Early work using iron surfaces was unsuccessful in yielding activation energies, probably because contaminants lowered the activity (5).

In the case of nickel, activation energies are higher on single crystal surfaces than on films and supported metal particles. Estimates are 88 kJ/mol on Ni(110) (6), 71 kJ/mol on Ni(111) (7), and 0 (8) and 30 (9) kJ/mol on Ni(100). On a Ni film 42 kJ/mol has been reported (5) and independent studies of methane activation by silica supported nickel yield similar barriers, 29 (10) and 25 (11) kJ/mol.

Activation of n-alkanes on platinum has been studied (12,13). Activation energies are about 46 kJ/mol on Pt(110) (13) and the inactivity of Pt(111) (12) has been interpreted to mean that n-alkane CH activation energies must be greater than 67 kJ/mol (13).

Because of various experimental difficulties in the early work, only the recently determined activation energies, 71 kJ/mol for Ni(111) and 30 kJ/mol for Ni(100) are likely to be accurate (5,9,13). The other values are in greater doubt.

Theoretical Method

The atom superposition and electron delocalization molecular orbital (ASED-MO) method (14) used in this paper is a semiempirical

theoretical approach which uses valence Slater orbitals (15) and experimental ionization potentials (16) as input data. The ASED-MO method is a simple way to predict certain molecular data from atomic data. Its structure and energy predictions are often quite accurate, but in general it is best used to establish and explain chemical trends.

Surfaces were modeled using the bulk-superimposable clusters in Figure 1. Atoms with which methane interacts directly in the transition state are shaded. Adsorption studies were performed assuming high-spin molecular orbital occupations with lower levels in the d band doubly occupied and upper levels singly occupied. The Fe₁₃ and Fe₁₄ clusters had 38 unpaired electrons, the Fe₁₁ cluster 30 and the Ni₁₀ and Pt₁₀ clusters 6 unpaired electrons. The cluster structures are bulk-superimposable and based on well-known lattice constants (17).

Methane activation on Fe(100) and (110) surfaces

Key numerical results are in Table I and transition state structures are in Figure 2. The activation energy for inserting an Fe(100) surface atom into a methane CH bond is 32 kJ/mol and occurs when the bond is stretched 0.36 Å. On a "roughened" surface site, consisting of an Fe ad-atom placed on top in a bulk-like position, the activation energy decreases slightly to 27 kJ/mol. The bonding in the transition state is best characterized as CH donation to the surface and the electronic structure for the ad-atom case is in Figure 3. This figure is representative of all other transition states discussed in this work. The stretching causes one of the 3-fold degenerate t_2 symmetry methane orbitals to become destabilized. Its bending of 22 deg away from the tetrahedral direction contributes further to the destabilization and also causes a small stabilization in one of the other t_2 orbitals. The lowest orbital is destabilized by the distortion. Interactions with the surface consist in a small stabilization of the lowest orbital and mixing of both of the upper orbitals from the t_2 set with the Fe orbitals to form clearly-defined C···H···Fe and C···Fe σ bonding orbitals. The main occupied antibonding counterpart orbital energy lies in the half-filled d band region and participation of the CH σ^* orbital in it removes almost all H contribution; the orbital has a C···Fe σ bonding character.

The transition state structures given in Figure 2 show how the methyl groups are tilted with respect to the two Fe(100) surfaces. The activated CH bonds are bent away from the tetrahedral directions, as are the newly-forming metal-carbon bonds. On these surfaces the deviations from the tetrahedral directions are nearly symmetric; numerical values for structure parameters are in Table I.

The total Mulliken overlap between the atom inserting into the CH bond and the surface cluster decreases when the atom is playing its activating role. Values given in Table I indicate a smaller decrease for the Fe/Fe(100) surface than for Fe(100). Furthermore, the bond order between the adsorbed Fe atom and the surface is less than between a surface atom and its neighbors.

The close-packed Fe(110) surface is much less reactive. The activation energy for site A is 118 kJ/mole and for site B it is 135 kJ/mol - see Figure 2 and Table I. The methyl tilts from vertical are less than for the (100) surface and this is symptomatic of increased steric repulsions with the closely-packed surface. The bending of the

activated CH bond away from the surface is greater than on Fe(100) and the Fe-C bonds are closer to the tetrahedral direction despite the greater Fe-C distances. There are significant changes in the bond order between the activating Fe atom and its neighbors. On the clean surface the bond order is higher than for Fe(100), indicating more near neighbors and stronger bonding. When the iron atom is activating CH, its overlap decreases more than for the (100) surface, lending further support to the idea that activating CH bonds weakens the metal bonding and that the stronger the metal bonding is, the more it must be perturbed and the weaker the activating ability of the surface. This appears to be borne out by the experimental results for (100) and (111) Ni.

Methane activation on Ni(111) and Pt(111) surfaces

Ni(111) is close-packed and the transition state structures are similar to those for Fe(110). The calculated activation energy, 64 kJ/mol, is close to 71 kJ/mol reported in (7), and provides a benchmark for our qualitative numbers. The effect of activation on the overlap of the active Ni atom with its neighbors is the same as for the close-packed Fe(110) surface.

The 43 kJ/mol activation energy calculated for Pt(111) is close to the experimentally determined value of about 46 kJ/mol for the (110) surface (13) and is smaller than implied by early studies of n alkanes on Pt(111) (12). We do not know precisely the reason for the disagreement. The calculations have uncertainty, but it is noted that the effects of transition state methane on the Pt-Pt bond order are more like those for the open Fe(100) surface than the close-packed Fe and Ni surfaces. We also note early work which stated Ni(111) was inactive compared to Ni(110) (6), yet very recent experiments yield a barrier for the Ni(111) surface close to our calculated value. Impurities may have passivated the (111) Ni surfaces in the early work.

Conclusions

The oxidative addition of methane to the iron, nickel, and platinum surfaces considered here is characterized by the insertion of a surface metal atom into a CH bond. Transition state CH bond stretches amount to around 0.4-0.5 Å. In the transition state two methane CH σ orbitals hybridize with the metal s and d band orbitals to form metal-H and metal-C bonds and the antibonding counterpart to these σ donation interactions is stabilized by mixing with the empty CH σ^* orbital to give additional C-metal bond order. Our finding of charge donation to the metal surfaces in most of the transition states conflicts with the conclusions of Saillard and Hoffmann (19) who used stylized structure models and Extended Hückel calculations, but never actually studied properties along reaction paths for activating methane.

We have found that the close-packed iron(110) surface is a much weaker CH activator than the more open (100) surface and that an ad-atom on the (100) surface is the most active site of all. These activities correlate with the inverse of the bond order between the activating surface atom and its neighbors. These bond orders undergo larger absolute and percentage changes when the activation energy is high, indicating a contribution to the barrier comes from a weakening of metal bonding at the transition state. Hydrogen atoms have been noted to weaken iron bonding in clusters while carbon atoms

strengthened iron overlaps (3). It is obvious that adsorption should affect metal bonding. The relative activation of close-packed and open surfaces toward methane could also have been anticipated.

Despite being close-packed, Ni(111) activates methane with a barrier half of that for Fe(110). Our calculated value is in good agreement with recent experiments and experimental estimates for Ni(100) and Ni films are less, as expected from the above theoretical results for iron. Pt(111) is predicted to be more active than Ni(111) and, therefore, much more active than Fe(110). An updated experimental look at Pt(111) is in order.

Acknowledgement

We are grateful to the Gas Research Institute for supporting this research.

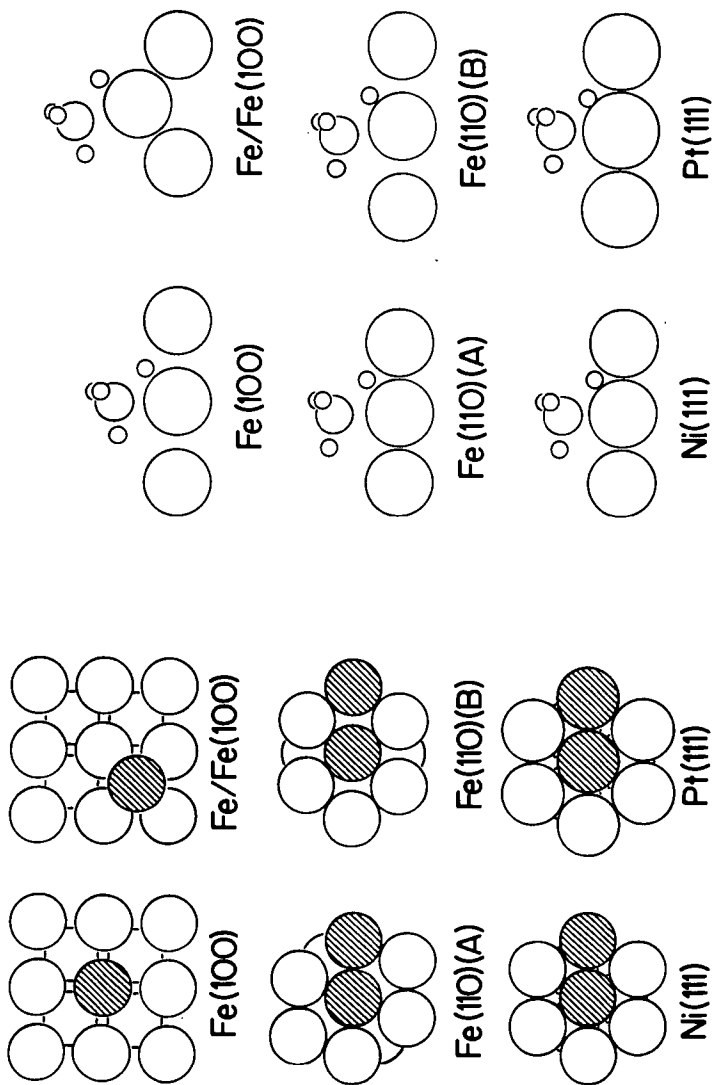
REFERENCES

1. Driscoll, D. J.; Lunsford, J. H. J. Phys. Chem. 1985, **89**, 4415.
2. Mehandru, S. P.; Anderson, A. B.; Brazdil, J. F. J. Phys. Chem. 1987, **00**, 0000.
3. Anderson, A. B. J. Am. Chem. Soc. 1977, **99**, 696.
4. Tibbetts, G. G. J. Cryst. Growth 1984, **66**, 632; 1985, **73**, 431.
5. Wright, P. G.; Ashmore, P. G.; Kemball, C. Trans. Faraday Soc. 1958, **54**, 1692.
6. Schouten, F. C.; Kaleveld, E. W.; Bootsma, G. A. Surf. Sci. 1977, **63**, 460.
7. Lee, M. B.; Yang, Q. Y.; Tang, S. L.; Ceyer, S. T. J. Chem. Phys. 1986, **85**, 1693.
8. Schouten, F. C.; Gijzeman, O. L. J.; Bootsma, G. A. Surf. Sci. 1979, **87**, 1.
9. Hamza, A. V.; Madix, R. J. Surf. Sci. 1987, **179**, 25.
10. Gaidai, N. A.; Babernich, L.; Gucci, L. Kinet. Katal. 1974, **15**, 974.
11. Kuijpers, E. G. M.; Jansen, J. W.; van Dillen, A. J.; Geus, J. W. J. Catal. 1981, **72**, 75.
12. Firment, L. E.; Somorjai, G. A. J. Chem. Phys. 1977, **66**, 2901.
13. Szuromi, P. D.; Engstrom, J. R.; Weinberg, W. H. J. Phys. Chem. 1985, **89**, 2497.
14. Anderson, A. B. J. Chem. Phys. 1975, **62**, 1187.
15. Clementi, E.; Raimondi, D. L. J. Chem. Phys. 1963, **38**, 2868.; Richardson, J. W.; Nieuwpoort, W. C.; Powell, R. R.; Edgell, W. F. J. Chem. Phys. 1962, **36**, 1057; Basch, H.; Gray, H. B. Theoret. Chim. Acta, 1966, **4**, 367.

16. Lotz, W. J. Opt. Soc. Am. 1970, 60, 206; Moore, C. E. Atomic Energy Levels, Natl. Bur. Std. (U.S.) Circ. 467 (U.S. Govt. Printing Office, Washington, D. C., 1958).
17. ASM Metals Reference Book, 2nd ed (American Society for Metals, Metals Park, Ohio, 1984).
18. Saillard, J.-Y.; Hoffmann, R. J. Am. Chem. Soc. 1984, 106, 2006.

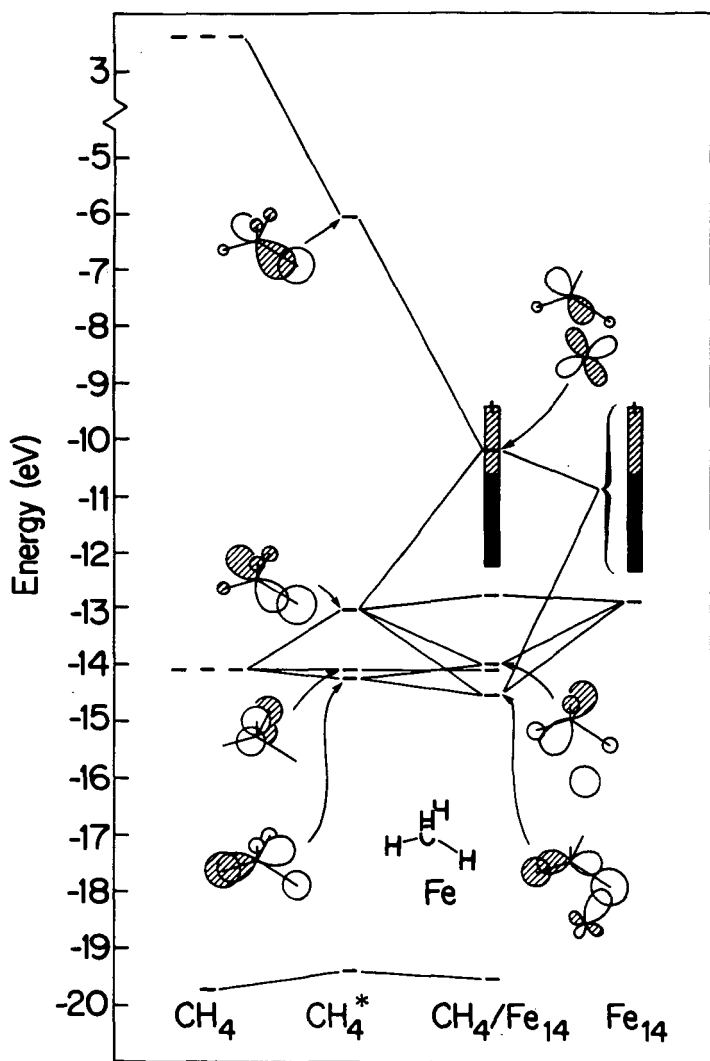
Table I. Calculated transition state properties. Structure parameters are with reference to Figure 2. The CH₃ tilt is from the vertical and bends are from the tetrahedral direction. The C-M bend and M-H and M-C distances are derived; other structure variables were optimized. The M-M_n overlap includes next-neighbor contributions and is calculated in the Mulliken definition.

surface	h _C (Å)	x _C (Å)	CH ₃ tilt (deg)	CH bend (deg)	CM bend (deg)	M-H(Å)	M-C(Å)	M-M _n overlap		E _a (kJ/mol)	
								value	change(%)		
Fe(100)	2.25	0.0	25	22	25	1.65	2.25	2.10	-9	0.36	32
Fe/Fe(100)	2.18	-0.57	37	22	22	1.57	2.25	2.13	-4	0.44	27
Fe(110) (A)	2.35	-0.05	12	34	11	1.66	2.35	2.39	-18	0.46	118
Fe(110) (B)	2.28	-0.30	16	35	8	1.58	2.30	2.37	-18	0.54	135
Ni(111)	2.15	-0.1	12	34	12	1.57	2.15	1.42	-17	0.51	64
Pt(111)	2.30	0.0	15	30	15	1.63	2.30	1.93	-8	0.36	43



1. Cluster models used for the calculations. Shaded atoms are those associated with methane in Figure 2.

2. Calculated transition state structures.



3. Orbital interactions between CH_4 and the ad atom on $\text{Fe}(100)$. Energy levels of distorted methane with the cluster removed are in the CH_4^* column. Orbitals in the shaded metal band region are half-filled.